

1 **Morphology of the Fibular Insertion of the Posterolateral Corner and Biceps Femoris Tendon**

2

3 Hirotaka Takahashi¹, MD, Goro Tajima¹, MD, PhD, Shuhei Kikuchi¹, MD, Jun Yan², PhD, Yoichi

4 Kamei¹, MD, PhD, Moritaka Maruyama¹, MD, PhD, Atsushi Sugawara¹, MD, PhD, Takaaki Saigo¹, MD,

5 Minoru Doita¹, MD, PhD

6 ¹Department of Orthopaedic Surgery, Iwate Medical University, Morioka, Japan

7 ²Department of Anatomy, Iwate Medical University, Morioka, Japan

8

9 Investigation performed at the Department of Anatomy, Iwate Medical University, Morioka, Japan

10

11 Corresponding author: Goro Tajima, MD, PhD.

12 Department of Orthopaedic Surgery, Iwate Medical University.

13 Address:

14 19-1 Uchimaru

15 Morioka, Iwate 020-8505, Japan

16 E-mail: goro.t@triton.ocn.ne.jp

17

18 Key words: Posterolateral corner, Fibular collateral ligament, Popliteofibular ligament, Fibular insertion

19

20 Running title:

21 Morphology of the fibular insertion of the posterolateral corner and biceps femoris tendon

22

23 Abbreviations:

24 PLC: posterolateral corner

25 FCL: fibular collateral ligament

26 PFL: popliteofibular ligament

27 3-D: three-dimensional

28 CT: computed tomography

29 A-P: antero-posterior

30

31 Financial Support

32 The authors received no external funding for this study.

33

34 Acknowledgements

35 This work was supported by JSPS KAKENHI Grant Number 15K01562. The authors wish to thank

36 Professors Jiro Hitomi and Yoichi Sato from the Department of Anatomy of Iwate Medical University for

37 their continuous support of this study. We are grateful for the support and encouragement of Kotaro
38 Fujino, MD, PhD, and Sanjuro Takeda, MD, PhD. We also thank Mr. Masayoshi Kamata from the
39 Department of Radiology of Iwate Medical University Hospital for his technical assistance.

40 **Introduction:**

41 The posterolateral corner (PLC) of the knee mainly consists of the fibular collateral ligament (FCL),
42 popliteus tendon (PT), and popliteofibular ligament (PFL) [16, 26]. The structure of the PLC acts as a
43 static stabilizer to resist varus and external rotation forces and posterior translation [17, 20, 31]. The
44 biceps femoris tendon acts a dynamic stabilizer to resist anterolateral-anteromedial rotatory instability of
45 the knee joint [32, 33]. Both the PLC and biceps femoris tendon are often damaged together with an
46 avulsion fracture of the fibular head [18], and injuries to both the PLC and biceps femoris tendon are
47 associated with severe rotatory instability [13].

48 Several studies have reported that injuries to the PLC are rarely found in isolation; however, they are
49 related to multiple ligament injuries, such as the combination of posterior cruciate ligament (PCL) injury
50 [4, 22]. Recent magnetic resonance imaging studies indicated that additional-posterolateral injuries were
51 present in 41-68% of patients with PCL injuries, and 37-62% of patients with anterior cruciate ligament
52 (ACL) injuries [6, 7, 13, 35]. In cases in which severe instability of PLC persisted, only isolated PCL
53 and/or ACL reconstruction has also been shown to be insufficient for stability [12]. It has also been
54 reported that if PLC injuries are left untreated, they may result in PCL and ACL graft failures, significant
55 impairment, including pain, meniscus tear, and osteoarthritis [9, 10, 13, 14, 15].

56 The treatment of PLC injuries remains controversial. Several studies have reported a higher rate of repair
57 failure compared with PLC reconstruction [1, 19, 28]. In contrast, a recent report showed that no

58 differences existed between reconstruction and repair groups with good tissue quality at the time of
59 surgery [21]. However, in cases of chronic PLC injuries, reconstruction of the PLC might be a more
60 reliable option in the setting of multiple ligament injuries [19, 21].

61 Several techniques for PLC reconstruction have been reported, such as using a fibular sling with 1 or 2
62 femoral tunnels [11, 25]. In recent years, anatomical reconstruction of the PLC has achieved superior
63 results [12, 20], and it was found to more favorably restore knee kinematics than non-anatomical
64 reconstruction in a biomechanical study [23]. However, tunnel positions, especially fibular tunnel
65 positions, have remained controversial.

66 Several anatomical studies of the femoral insertion of the PLC and their optimal tunnel position have
67 been reported [2, 5, 16, 24, 26, 30]; however, little has been mentioned about the fibular side [2, 24, 27,
68 34]. To precisely repair or anatomically reconstruct the PLC, it is necessary to define the optimal
69 positions of the FCL, PFL, and biceps femoris tendon insertions, and relations between the characteristic
70 features of the fibular head and those insertions.

71 The aim of this study was to clarify the fibular insertion of the FCL, PFL, biceps femoris tendon, and
72 related osseous landmarks on three-dimensional (3-D) images. The hypothesis was that characteristic
73 features of their insertions can be identified and that they are consistent.

74

75 **Materials and Methods:**

76 Twenty-one unpaired human cadaveric knees (sixteen from males and five from females), with no severe
77 macroscopic or traumatic changes, were used in this study. The mean age at the time of death was $77.8 \pm$
78 9.8 years (range: 63-95 years). All cadavers were placed in 10% formalin and preserved in 50% alcohol
79 for 6 months.

80 Dissection began with removal of the skin and soft subcutaneous tissue on the lateral side of the knee.
81 The iliotibial tract was cut on the proximal side and turned over by the tibial attachment. After the
82 removal of the iliotibial tract, the biceps femoris tendon was identified and cut on the proximal side of the
83 fibular insertion. The biceps femoris tendon was peeled off the fibular insertion, and then the FCL and
84 PFL were identified and observed grossly. They were cut in the midsubstance, elevated from the fibular
85 head, and outlined using a fine 1.0-mm-diameter drill.

86

87 *Three-dimensional measurement and visualization*

88 Knees were scanned using a 16-row multislice computed tomography (CT) scanner (ECLOS; Hitachi
89 Medical Corporation, Tokyo, Japan). Axial plane images with 0.5-mm slices were obtained and saved as
90 Digital Imaging and Communications in Medicine (DICOM) data. All digital data imaging were uploaded
91 to dedicated software (Mimics version 15.0 and MedCAD module; Materialise N.V., Belgium), and 3-D
92 images of the knee were created. On the 3-D images, the morphology of the fibular head, the fibular
93 insertions of the FCL, PFL, and biceps femoris tendon, and these surface areas were analyzed. The center

94 of the insertions of the FCL, PFL, and biceps femoris tendon was defined automatically as the centroid of
95 their area using the software mentioned. The linear distance between the center of the fibular insertion of
96 the FCL or PFL and the apex of related structures was measured on 3-D images. The linear distance
97 between the center of the FCL and PFL insertions was also measured.

98 The coordinates of the center of the fibular head insertion of the FCL and PFT were mapped on two
99 squares with an antero-posterior (A-P) and lateral view on the 3-D images. The coordinate planes were
100 created using the tibial plane [29]. With an A-P view, the maximum medial-lateral diameter of the length
101 between the most medial and lateral points of the fibular head was used as a standard (100%). With a
102 lateral view, the maximum A-P diameter of the length between the most anterior and posterior points was
103 used as a standard (100%) (Figs. 3a and 3b).

104 These cadavers were donated to Iwate Medical University for education and research purposes, and
105 informed consent for donation was obtained from each patient and their family prior to death. This
106 cadaveric study was approved by the Ethical Committees of Iwate Medical University (IRB: H27-99).

107 The accuracy of the length and area measurements was less than 0.1 mm and 0.1 mm², respectively.

108 When comparing the accuracy of 3-D models generated from CT with the optical scan, the average error
109 was 0.65 ± 0.31 mm or around one-third of the pixel size [8]. The tolerance and margin of error of CT
110 measurements (according to the manufacturer) were ± 0.39 mm. The distribution of each variable was

111 checked for normality using the Kolmogorov–Smirnov test. Statistical data were calculated using SPSS
112 v.20.0 (IBM, Armonk, NY, USA).

113

114 **Results:**

115 *Macroscopic findings*

116 The insertions of the FCL, PFL, and biceps femoris tendon were clearly identified in all knees. The lateral
117 point of the fibular head and fibular styloid process could be identified easily as osseous landmarks of the
118 fibular head by palpation in all knees. However, the anterior point was difficult to palpate because various
119 soft tissues, such as the proximal tibiofibular joint ligament and peroneus longus muscle, were firmly
120 attached around it. The lateral and posterior aspects of the fibular head were also identified. The biceps
121 femoris tendon was firmly attached to the lateral aspect of the fibular head surrounding the FCL (Fig. 1).
122 The FCL originated from the posterior slope of the lateral epicondyle, and inserted from the center of the
123 lateral aspect to the lateral point of the fibular head intersecting the biceps femoris tendon. The PFL
124 originated from the musculo-tendinous junction of the PT, and inserted to around the fibular styloid
125 process (Fig. 2a).

126

127 *3-D measurements of fibular insertions of the FCL and PFL*

128 Fibular insertions of both the FCL and PFL, especially the PFL, varied markedly in size. The mean
129 surface areas of the FCL and PFL fibular insertions were $100.1 \pm 29.5 \text{ mm}^2$ and $18.5 \pm 7.2 \text{ mm}^2$,
130 respectively. Quantitative data are summarized in Table 1.

131

132 *Locations and coordinates with A-P and lateral views on 3-D images*

133 Coordinates for centers of the FCL and PFL fibular insertions were obtained. With an A-P view, the
134 centers of fibular insertion of the FCL were $x = 94.8 \pm 2.7\%$ and $y = 57.4 \pm 8.8\%$, and those of the PFL
135 were $x = 70.2 \pm 6.7\%$ and $y = 5.7 \pm 3.2\%$, respectively. With a lateral view, the centers of fibular head
136 insertion of the FCL were $x = 52.4 \pm 5.6\%$ and $y = 62.8 \pm 7.5\%$, and those of the PFL were $x = 82.8 \pm$
137 4.9% and $y = 5.9 \pm 3.4\%$, respectively (Figs. 3c and 3d). Quantitative data are summarized in Table 2.

138

139 *Characteristic features of the fibular head on 3-D images*

140 On 3-D images, the fibular head consisted of three aspects: the lateral aspect, posterior aspect, and
141 proximal tibiofibular facet. The shape of the fibular head was pyramidal, with the fibular styloid process,
142 and anterior, lateral, and medial points. Four points were labeled F, A, L, and M, representing the fibular
143 styloid process, and anterior, lateral, and medial points of the fibular head, respectively, and the sides
144 between these points were labeled FA, FL, FM, AL, AM and LM, and measured (Fig. 4). The distances of
145 FA, FL, FM, AL, AM, and LM were $27.4 \pm 2.0 \text{ mm}$, $24.7 \pm 2.8 \text{ mm}$, $24.6 \pm 4.5 \text{ mm}$, $19.6 \pm 2.7 \text{ mm}$, 27.3

146 ± 2.5 mm, and 29.4 ± 3.0 mm, respectively. The distances of each side were nearly equal, and the shape
147 of the fibular head was similarly triangular and pyramidal in appearance.

148

149 *Positional relationships among the FCL, PFL, and related osseous landmarks*

150 On 3-D images, the lateral point of the fibular head, the fibular styloid process, and also the anterior point
151 of the fibular head, which was not clearly identified based on macroscopic findings, could be identified as
152 osseous landmarks. The insertion of the FCL was attached from a lateral point to the center of the lateral
153 aspect of the fibular head. The distances between the centers of the FCL insertion and anterior or lateral
154 point of the fibular head, or the fibular styloid process, were 18.1 ± 1.9 mm, 6.3 ± 1.1 mm, and 21.6 ± 2.5
155 mm, respectively. The insertion of the PFL was attached from the fibular styloid process to the posterior
156 aspects. The distances between the centers of the PFL insertion and anterior or lateral point of the fibular
157 head, or the fibular styloid process, were 25.2 ± 2.9 mm, 24.2 ± 2.2 mm and 2.3 ± 1.0 mm, respectively.

158 The distance between the centers of the FCL and PFL insertions was 20.4 ± 2.6 mm. Quantitative data are
159 summarized in Table 1.

160

161 **Discussion:**

162 The most important findings of this study were the clarifications of the relationships between the
163 characteristic features of the fibular head and insertions of the FCL, PFL, and biceps femoris tendon on

164 3-D images. The shape of the fibular head was similar to regular triangular and pyramidal with sides
165 approximately 25 mm long. In appearance as a unique structure. The insertions of the FCL, PFL, and
166 biceps femoris tendon were inserted from the center of the lateral aspect to the lateral point of the fibular
167 head, from the fibular styloid process to the posterior aspect, and to the lateral aspect surrounding the
168 FCL, respectively. The relationships between the characteristic features of the fibular head and their
169 insertions were consistent.

170 This study provided detailed data concerning the surface areas of the fibular insertions of both the FCL
171 and PFL that varied markedly in size. This finding regarding the fibular insertion of the FCL was similar
172 to the observation by Branch et al. using a calibrated stylus utilizing standard system software, who
173 reported that the surface area of the fibular insertion of the FCL averaged 87 mm^2 , although they did not
174 mention about the insertion of the PFL [2]. In contrast, LaPrade et al. only reported that the surface area
175 of the fibular insertion of the FCL averaged 48 mm^2 using a video motion analysis capture system [16].
176 Using the Isotrak digitizing system, Brinkman et al. found that the surface area of the fibular insertion of
177 the FCL averaged 35 mm^2 and the PFL averaged 17 mm^2 [3]. Their findings of the PFL were similar to
178 this results; however, the FCL was smaller than in the present study. This difference might be due to the
179 method for identification of the fibular insertion of the FCL, which is surrounded by firm attachments to
180 the biceps femoris tendon, or the measurement system.

181 This study revealed accurate coordinate positions of centers of the fibular insertion of the FCL and PFL
182 with A-P and lateral views on 3-D images. No studies have mentioned the positions of the centers of the
183 FCL and PFL fibular insertions using 3-D images. This study can shows the importance of considering
184 individual difference in the size of the fibular head, and so it may aid in the determination of an accurate
185 tunnel position during surgery.

186 This study also revealed the distance between the centers of the FCL or PFL and their osseous landmarks:
187 the anterior or lateral point of the fibular head, or the fibular styloid process. The distance between the
188 FCL or PFL and the fibular styloid process was similar to the observation by Pierrini et al., who reported
189 that the distances between the FCL or PFL and the fibular styloid process were 17.6 ± 4.1 and 4.8 ± 2.3
190 mm, respectively, although they did not mention about anterior and lateral points [26]. LaPrade et al.
191 reported that the distances between the FCL and anterior point or the fibular styloid process were 8.2 and
192 28.4 mm, respectively. They also reported that the distance between the PFL and fibular styloid process
193 was 2.8 mm. Their results regarding the distance between the FCL or PFL and the fibular styloid process
194 were similar to this study; however, the distance between the FCL and anterior point of the fibular head
195 was shorter than this result [16]. Several studies have described the osseous landmarks for the fibular
196 insertion of the FCL and PFL in relation to the anterior point of the fibular head and the fibular styloid
197 process [3, 16, 26]; however, no reports have mentioned about the lateral point of the fibular head as an
198 osseous landmark. Although the anterior point was not identified clearly by examination of the gross

199 anatomy in this study, the lateral point and fibular styloid process were clearly identified in all knees.

200 Therefore, the lateral point and fibular styloid process may be more useful osseous landmarks than the

201 anterior point for identification of their insertions intraoperatively.

202 More importantly, the relationships between the characteristic features of the fibular head and insertions

203 of the FCL, PFL, and biceps femoris tendon were consistent. We also present a simplified schematic

204 diagram of the fibular head showing a pyramidal shape as a unique structure. At the time of surgery, it

205 can be difficult to identify their fibular insertions, because the fibular head is relatively small, in

206 combination with an avulsion fracture, various soft tissue injuries and scar formation after PLC injuries.

207 Therefore, we believe that the simple characteristic feature of the fibular head which we showed, can be

208 the most useful osseous landmarks and may assist surgeons to confirm the accurate position of the fibular

209 insertions of the PLC during surgery.

210 This study had several limitations. Firstly, cadavers with a mean age of 77.8 years were used. Even

211 though no specimens had severe macroscopic degenerative or traumatic changes, it cannot be ruled out

212 that degenerative changes may have affected identification of the osseous landmarks. Secondly, a

213 comparatively small number of specimens were investigated. Thirdly, formalin-preserved cadavers, with

214 which it is occasionally difficult to identify fine structures of soft tissues, were used. Fourthly, this study

215 used an accurate method of 3-D measurement and visualization; however, it also cannot be ruled out that

216 human dissection and subjective decisions regarding the insertion site of the FCL, PFL, and biceps
217 femoris tendon introduced error and bias.

218 The clinical relevance of this study is that it improves understanding of the anatomy of the insertions of
219 the FCL, PFL and biceps femoris tendon, and assists surgeons in performing precise repair or anatomical
220 reconstruction of the PLC.

221

222 **Conclusion**

223 This study showed that the relationships between the characteristic features of the fibular head and
224 insertions of the FCL, PFL, and biceps femoris tendon were consistent. The clinical relevance of this
225 study is that it improves understanding of the anatomy of the insertions of the PLC and biceps femoris
226 tendon.

227 **References:**

- 228 1 Black BS, Stannard JP (2015) Repair versus reconstruction in acute posterolateral instability of the knee.
229 Sports Med Arthrosc 23: 22-26
- 230 2 Branch EA, Anz AW (2015) Distal insertions of the biceps femoris: a quantitative analysis. Orthop J
231 Sports Med. doi: 10.1177/2325967115602255.
- 232 3 Brinkman JM, Schwering PJ, Blankevoort L, Koolos JG, Luites J, Wymenga AB (2005) The insertion
233 geometry of the posterolateral corner of the knee. J Bone Joint Surg Br 87: 1364-1368
- 234 4 Collins MS, Bond JR, Crush AB, Stuart MJ, King AH, Levy BA (2015) MRI injury patterns in
235 surgically confirmed and reconstructed posterolateral corner knee injuries. Knee Surg Sports Traumatol
236 Arthrosc 23: 2943-2949
- 237 5 Gali JC, Bernardes Ade P, dos Santos LC, Ferreira TC, Almagro MA, da Silva PA (2016) Tunnel
238 collision during simultaneous anterior cruciate ligament and posterolateral corner reconstruction. Knee
239 Surg Sports Traumatol Arthrosc 24: 195-200
- 240 6 Geeslin AG, LaPrade RF (2010) Location of bone bruises and other osseous injuries associated with
241 acute grade III isolated and combined posterolateral knee injuries. Am J Sports Med 38: 2502-2508
- 242 7 Geeslin AG, LaParde RF (2011) Outcomes of treatment of acute grade-III isolated and combined
243 posterolateral knee injuries. J Bone Joint Surg Am 93: 1672-1683

- 244 8 Gelaude F, Vander Sloten J, Lauwers B (2008) Accuracy assessment of CT-based outer surface femur
245 meshes. *Comput Aided Surg* 13: 188-199
- 246 9 Harner CD, Höher J, Vogrin TM, Carlin GJ, Woo SL (1998) The effects of a popliteus muscle load on
247 in situ forces in the posterior cruciate ligament and on knee kinematics. A human cadaveric study. *Am J*
248 *Sports Med* 26: 669-673
- 249 10 Kannus P (1989) Nonoperative treatment of grade II and III sprains of the lateral ligament
250 compartment of the knee. *Am J Sports Med* 17: 83-88
- 251 11 Kim JG, Ha JG, Lee YS, Yang SJ, Jung JE, Oh SJ (2009) Posterolateral corner anatomy and its
252 anatomical reconstruction with single fibula and double femoral sling method: anatomical study and
253 surgical technique. *Arch Orthop Trauma Surg* 129: 381-385
- 254 12 Kuzuma SA, Chow RM, Engasser WM, Stuart MJ, Levy BA (2014) Reconstruction of the
255 posterolateral corner of the knee with achilles tendon allograft. *Arthosc Tech* 3: 393-398
- 256 13 LaPrade RF, Terry GC (1997) Injuries to the posterolateral aspect of the knee. Association of anatomic
257 injury patterns with clinical instability. *Am J Sports Med.* 25: 433-438.
- 258 14 LaPrade RF, Terry GC, Montgomery RD, Curd D, Simmons DJ (1998) The effects of aggressive
259 notchplasty on the normal knee in dogs. *Am J Sports Med* 26: 193-200

260 15 LaPrade RF, Muench C, Wentorf F, Lewis JL (2002) The effect of injury to the posterolateral
261 structures of the knee on force in a posterior cruciate ligament graft: a biomechanical study. *Am J Sports*
262 *Med* 30: 233-238

263 16 LaPrade RF, Ly TV, Wentorf FA, Engebretsen L (2003) The posterolateral attachments of the knee: a
264 qualitative and quantitative morphologic analysis of the fibular collateral ligament, popliteus tendon,
265 popliteofibular ligament, and lateral gastrocnemius tendon. *Am J Sports Med* 31: 854-860

266 17 LaPrade RF, Johansen S, Wentorf FA, Engebretsen L, Esterberg JL, Tso A (2004) An analysis of an
267 anatomical posterolateral knee reconstruction: an in vitro biomechanical study and development of a
268 surgical technique. *Am J Sports Med* 32: 1405-1414.

269 18 Lee J, Papakostantinou O, Brookenthal KR, Trudell D, Resnick DL (2003) Arcuate sign of
270 posterolateral knee injuries: anatomic, radiographic, and MR imaging data related to patterns of injury.
271 *Skeletal Radiol* 32: 619–627

272 19 Levy BA, Dajani KA, Morgan JA, Shah JP, Dahm DL, Stuart MJ (2010) Repair versus reconstruction
273 of the fibular collateral ligament and posterolateral corner in the multiligament-injured knee. *Am J Sports*
274 *Med* 38: 804-809

275 20 McCarthy M, Camarda L, Wijicks CA, Johansen S, Engebretsen L, LaPrade RF (2010) Anatomic
276 posterolateral knee reconstructions require a popliteofibular ligament reconstruction through a tibial
277 tunnel. *Am J Sports Med* 38: 1674-1681

278 21 McCarthy M, Ridley TJ, Bollier M, Wolf B, Cook S, Amendola A (2015) Posterolateral knee
279 reconstruction versus repair. *The Iowa Orthopaedic Journal* 35: 20-25

280 22 McKean D, Yoong P, Yanny S, Thomee E, Grant D, Teh JL, Mansour R (2015) The popliteal fibular
281 ligament in acute knee trauma: patterns of injury on MR imaging. *Skeletal Radiol* 44 (10): 1413-1419

282 23 Miyatake S, Kondo E, Tsai TY, Hirschman M, Halewood C, Jakobsen BW, Yasuda K, Amis AA
283 (2011) Biomechanical comparisons between 4-strand and modified Larson 2-strand procedures for
284 reconstruction of the posterolateral corner of the knee. *Am J Sports Med* 39: 1462–1469

285 24 Osti M, Tschann P, Künzel KH, Benedetto KP (2013) Posterolateral corner of the knee: microsurgical
286 analysis of anatomy and morphometry. *Orthopedics* 36: 1114-1120

287 25 Panzica M, Janzik J, Bobrowitsch E, Krettek C, Hawi N, Hurschler C, Jagodzinski M (2015)
288 Biomechanical comparison of two surgical techniques for press-fit reconstruction of the posterolateral
289 complex of the knee. *Arch Orthop Trauma Surg* 135: 1579-1588

290 26 Pietrini SD, LaPrade RF, Griffith CJ, Wijdicks CA, Ziegler CG (2009) Radiographic identification of
291 the primary posterolateral knee structures. *Am J Sports Med* 37: 542-551

292 27 Song GY, Zhang H, Zhang J, Li Y, Feng H (2015) Anatomical popliteofibular ligament reconstruction
293 of the knee joints: an all-arthroscopic technique. *Knee Surg Sports Traumatol Arthrosc* 23: 2925-2929

294 28 Stannard JP, Brown SL, Farris RC, McGwin G Jr, Volgas DA (2005) The posterolateral corner of the
295 knee: Repair versus reconstruction. *Am J Sports Med* 33: 881-888

296 29 Tajima G, Nozaki M, Iriuchishima T, Ingham SJ, Shen W, Smolinski P, Fu FH (2009) Morphology of
297 the tibial insertion of the posterior cruciate ligament. *J Bone Joint Surg Am* 91: 859-866

298 30 Takeda S, Tajima G, Fujino K, Yan J, Kamei Y, Maruyama M, Kikuchi S, Doita M (2015)
299 Morphology of the femoral insertion of the lateral collateral ligament and popliteus tendon. *Knee Surg*
300 *Sports Traumatol Arthrosc* 23: 3049-3054

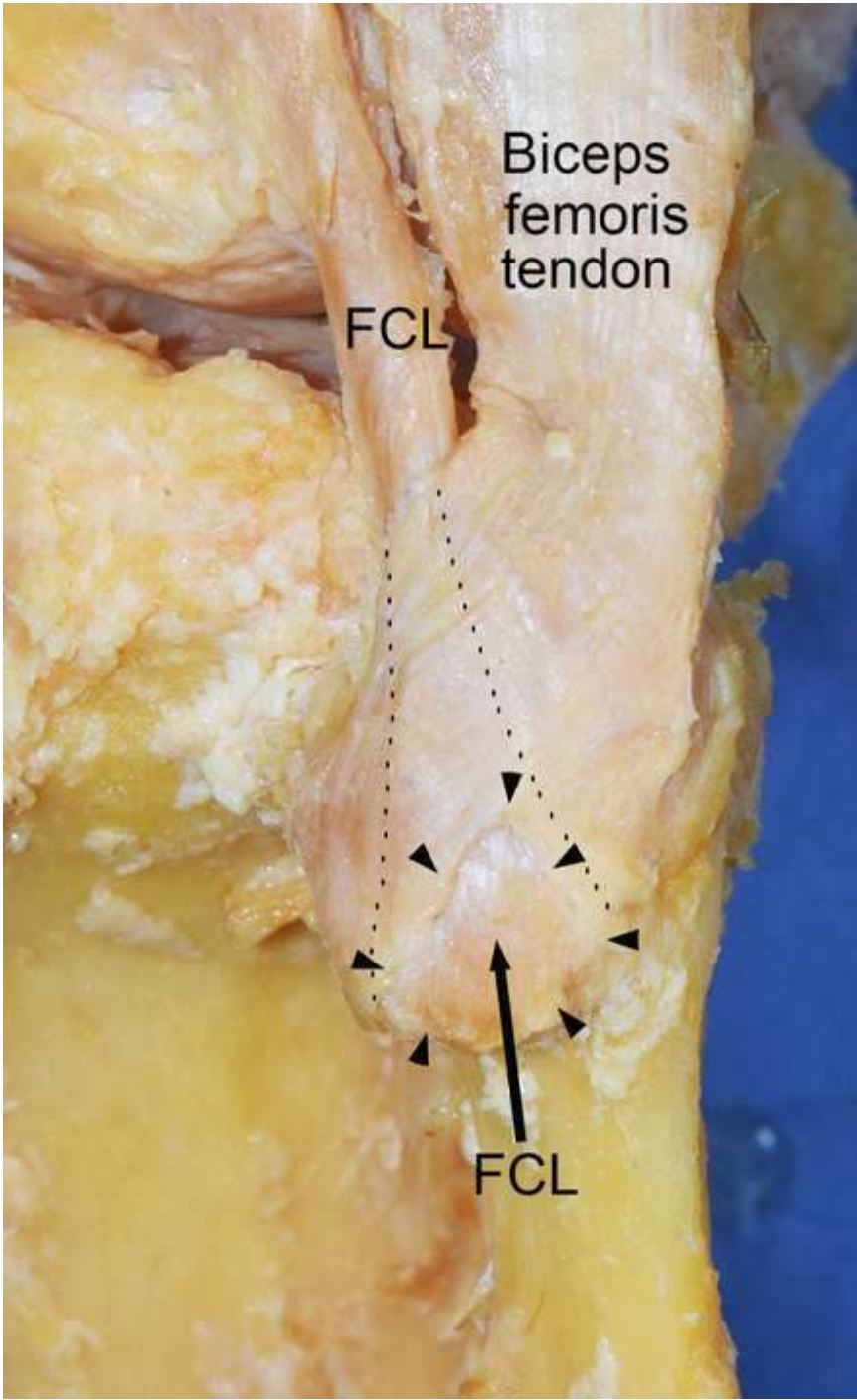
301 31 Thaunat M, Pioger C, Chatellard R, Conteduca J, Khaleel A, Sonnery-Cottet B (2014) The arcuate
302 ligament revisited: role of the posterolateral structures in providing static stability in the knee joint. *Knee*
303 *Surg Sports Traumatol Arthrosc* 22: 2121-2127

304 32 Terry GC, LaPrade RF (1996) The biceps femoris muscle complex at the knee. Its anatomy and injury
305 patterns associated with acute anterolateral-anteromedial rotatory instability. *Am J Sports Med* 24: 2-8

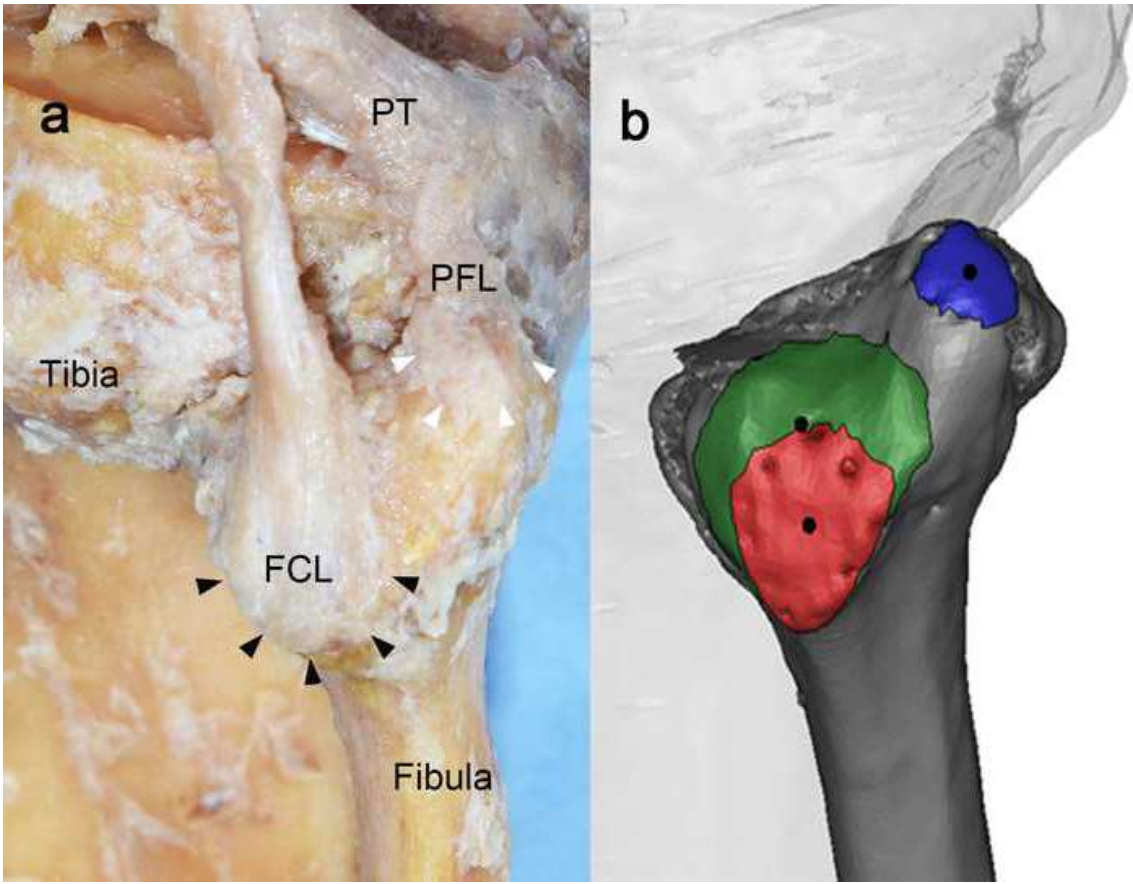
306 33 Tubbs RS, Caycedo FJ, Oakes WJ, Salter EG (2006) Descriptive anatomy of the insertion of the
307 biceps femoris muscle. *Clinical Anatomy* 19: 517-521

308 34 Wechter JF, Bohm KC, Macalena JA, Sikka RS, Tompkins M (2015) Part II: The 50/60 fibular tunnel
309 trajectory for posterolateral corner reconstruction in a cadaver model. *Knee Surg Sports Traumatol*
310 *Arthrosc* 23: 1895-1899

311 35 Yoon KH, Lee JH, Bae DK, Song SJ, Chung KY, Park YW (2011) Comparison of clinical results of
312 anatomic posterolateral corner reconstruction for posterolateral rotatory instability of the knee with or
313 without popliteal tendon reconstruction. *Am J Sports Med* 39: 2421-2428



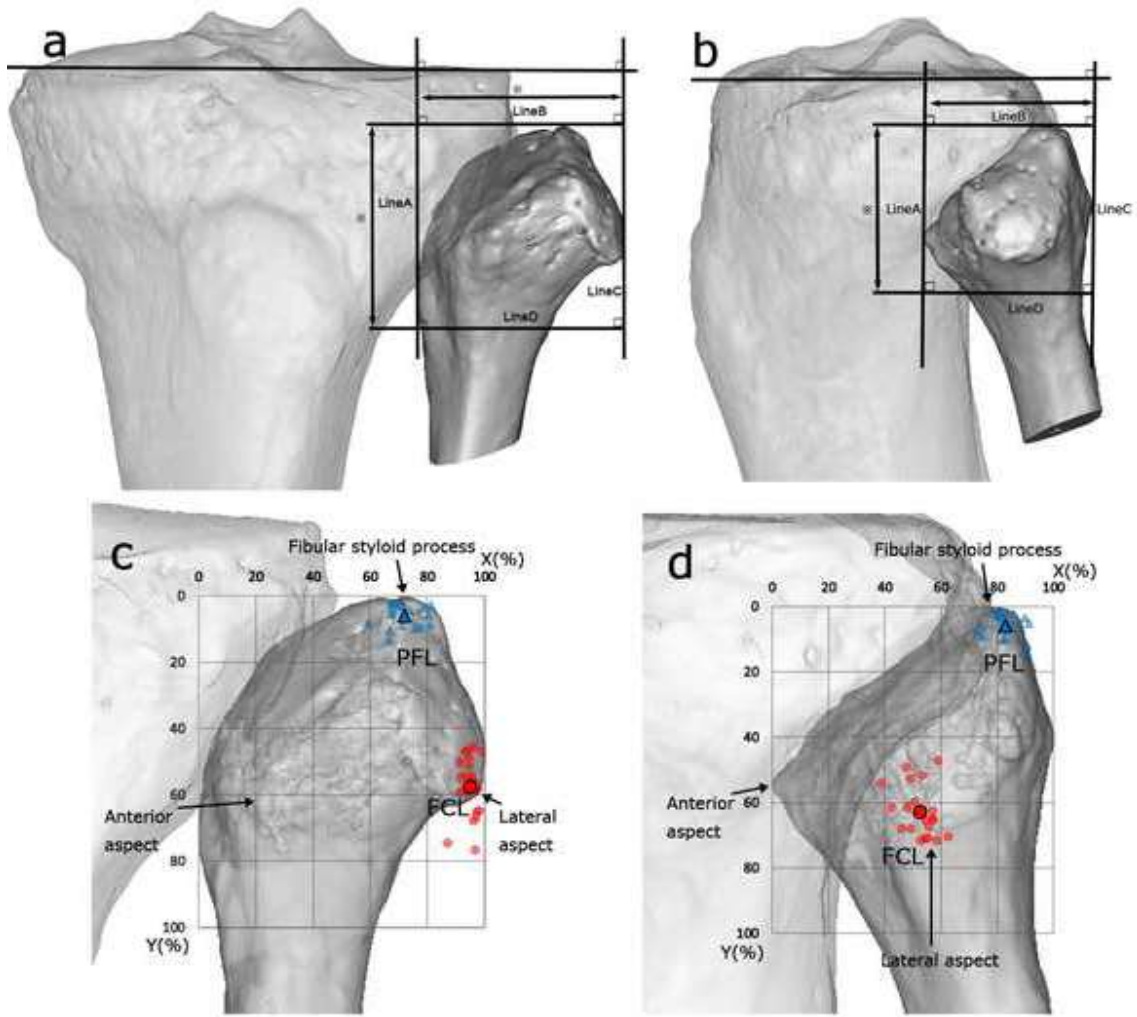
315 Fig.1 Macroscopic findings with a lateral view of the left knee, showing the biceps femoris tendon and
316 fibular collateral ligament (FCL). The biceps femoris tendon was firmly attached to the lateral aspect of
317 the fibular head surrounding the FCL. The black arrowheads show the insertion area of the FCL.



318

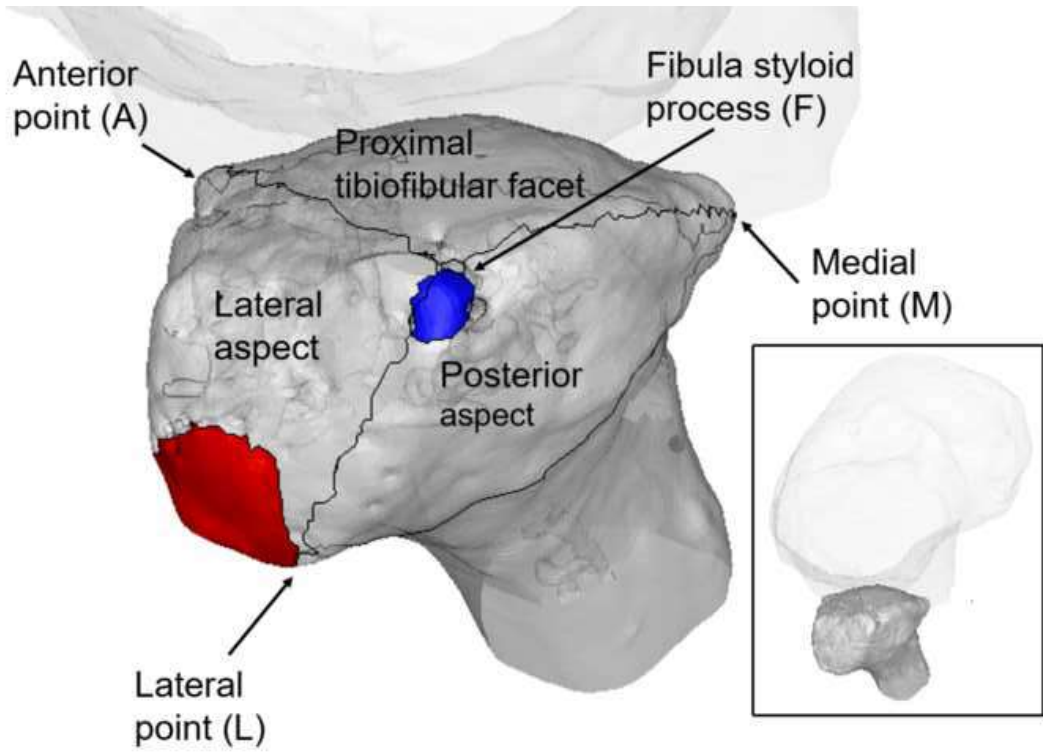
319 Fig. 2-a: Macroscopic findings with a lateral view of the left knee. The black arrowheads show the
320 insertion area of the FCL and the white arrowheads show the insertion area of the popliteofibular
321 ligament (PFL).

322 Fig. 2-b: The insertion areas of the fibular head on three-dimensional (3-D) images. The red area shows
323 the fibular insertion area of the FCL, the blue area shows the fibular insertion area of the PFL, and the
324 green area shows the fibular insertion area of the biceps femoris tendon. The black circles indicate the
325 centers of their insertions.



327 Fig. 3 a and b: Original coordinate planes with squares. Squares with reference lines A, B, C, and D were
328 drawn with antero-posterior and true lateral views. *Line A* A line which contacts at the most medial and
329 anterior points of the fibular head was drawn perpendicular to the tibial plane. *Line B* Contact points at
330 the most proximal point of the fibular head were plotted parallel to the tibial plane. *Line C* Contact points
331 at the most lateral and posterior points of the fibular head were plotted perpendicular to the tibial plane.
332 *Line D* A line parallel to the tibial plane was drawn to create squares. The asterisk indicates the standard
333 length (as 100%) for lines A and C and for lines B and D.

334 Fig. 3 c and d: Coordinates for the centers of the FCL (red circle) and PFL (blue triangle) are shown with
335 an antero-posterior (A-P) view (Fig.3. c) and a lateral view (Fig.3. d). A large red circle and blue triangle
336 indicate the mean centers of the FCL and PFL. The X-axis is the top of the square, the Y-axis is the
337 medial perpendicular line on the squares, and the origin of the coordinate axes is the point of intersection
338 between the uppermost line and medial perpendicular lines. The coordinates of the center of the femoral
339 insertion of the FCL and PFL were plotted on squares with A-P and lateral views.



341 Fig. 4: Characteristic features of the fibular head on a 3-D image with a proximal view. The fibular head
342 consists of three aspects: lateral aspect, posterior aspect, and tibiofibular facet. The red area indicates the
343 fibular insertion area of the FCL and the blue area indicates fibular insertion area of the PFL. _____

Table 1

Quantitative measurement of the FCL and PFL and related bone landmarks

	FCL	PFL
Distance from the anterior point (mm)	18.1 ± 1.9 (15.0-21.8)	25.2 ± 2.9 (18.0-28.3)
Distance from the fibular styloid process (mm)	21.6 ± 2.5 (15.0-25.2)	2.3 ± 1.0 (0.8-4.1)
Distance from the lateral point (mm)	6.3 ± 1.1 (4.4-8.9)	24.2 ± 2.2 (17.4-27.6)
Distance from the FCL (mm)		20.4 ± 2.6 (14.6-24.5)
Distance from the PFL (mm)	20.4 ± 2.6 (14.6-24.5)	
Mean surface area (mm ²)	100.1 ± 29.5 (63.9-175.9)	18.5 ± 7.2 (6.2-30.2)

Data are presented as mean ± SD, range

Table 2

Locations and coordinates on A-P and lateral views of 3-D images

	The center of the FCL fibular head insertion (%)	The center of the PFL fibular head insertion (%)
X (A-P view)	94.8 ± 2.7% (87.2-98.5)	70.2 ± 6.7% (58.8-81.4)
Y (A-P view)	57.4 ± 8.8% (45.7-76.7)	5.7 ± 3.2% (2.2-13.3)
X (lateral view)	52.4 ± 5.6% (38.9-62.5)	82.8 ± 4.9% (73.1-91.3)
Y (lateral view)	62.8 ± 7.5% (47.1-71.7)	5.9 ± 3.4% (1.9-14.2)

Data are presented as mean ± SD, range